

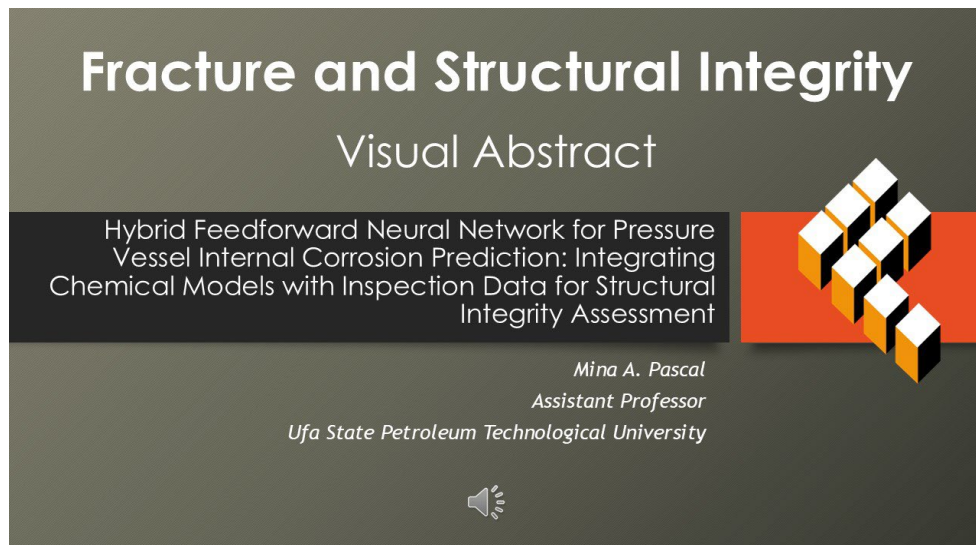


Hybrid feedforward neural network for pressure vessel internal corrosion prediction: integrating chemical models with inspection data for structural integrity assessment

Mina A. Pascal

Ufa State Petroleum Technological University, Ufa, Russian Federation

Mina.apascal@gmail.com, <https://orcid.org/0000-0002-6849-0283>



Citation: Pascal, M. A., Hybrid feedforward neural network for pressure vessel internal corrosion prediction: integrating chemical models with inspection data for structural integrity assessment, *Fracture and Structural Integrity*, 76 (2026)49-66.

Received: 06.12.2025

Accepted: 05.01.2026

Published: 06.01.2026

Issue: 04.2026

Copyright: © 2026 This is an open access article under the terms of the CC-BY 4.0, which permits unrestricted use, distribution, and reproduction in any medium, provided the original author and source are credited

KEYWORDS. Hybrid models, Neural network Model, Corrosion rate prediction, Pressure vessel, Structure integrity, Physics-informed modelling.

INTRODUCTION

The prediction and detection of corrosion in oil and gas pressure vessels are critical challenges in asset integrity management. Corrosion-induced failures result in significant economic losses, environmental hazards, and potential safety incidents, with repair and replacement costs often exceeding millions of dollars per incident [1]. Pressure vessels operating in harsh industrial environments are continuously exposed to aggressive chemicals, elevated temperatures, and variable pH conditions that progressively degrade material properties, reducing mechanical strength and potentially leading to catastrophic structural failure [2]. Accurate corrosion prediction models are therefore essential for proactive maintenance planning, ensuring operational reliability, and extending asset service life.

Corrosion prediction models have been the most reported approaches for corrosion risk mitigation, with the objective of improving maintenance planning and reducing failure risks [3]. The models utilize record keeping, in situ experimental observations, and inspection data to quantify material degradation in terms of corrosion rates, extents, and locations [4]. Modern corrosion prediction approaches use many different models with different assumptions and strengths. Empirical models based on power-law formulations using historical data are straightforward but not robust to complex conditions [5].



Conventional machine learning (ML) and deep learning (DL) algorithms trained on large datasets can be effective in recognizing patterns, but require substantial computational resources. Physics-informed simulations (i.e., finite element models (FEM)) provide accurate predictions but require high computing power. Hybrid methodologies that integrate machine learning (ML) methods with physics-based models, risk-based inspection (RBI) frameworks, and electrochemical modeling and simulations can yield improved predictive capability and performance [6].

Neural networks (NN) and similar methods are often used to estimate the corrosion rate and assess the integrity of pressure vessels. These hybrid approaches combine data-driven neural networks with physics-based constraints to improve prediction accuracy. Other compatible methods include computational fluid dynamics (CFD), finite element modelling (FEM), and physics-based modelling, which allow for rapid or accurate estimation of corrosion [7]. Hybrid modelling has been demonstrated for all types of corrosive mechanisms, including uniform corrosion, pitting, and stress corrosion cracking, and can adapt to various operational and environmental conditions [8].

Hybrid NN methods offer several advantages, particularly the ability to integrate physics-based models to improve prediction accuracy. Hybrid approaches for modeling CO₂ and O₂ corrosion rates in pipelines have been developed to account for local phenomena such as flow patterns and mass transfer, and hybrid PCA-MLP models have been applied to subsea pipeline corrosion in heavy multiphase flow conditions [9]. Theory-driven neural network models have also been developed to predict burst pressures of corroded pipelines by incorporating physical constraints into the network architecture [10]. Furthermore, hybrid methods combining ANNs with advanced algorithms have been used to predict corrosion characteristics of subsea pipelines under uncertain operating conditions [11].

In this study, a hybrid model based on chemical corrosion theory and feedforward neural networks (FNNs) was developed. The model is constructed with a physics-informed design using common process data, and corrosion rates and uncertainty estimates are generated via Monte Carlo dropout. The thickness data obtained in these inspections are used to update the prediction and to estimate the remaining useful life (RUL) of the components based on the proposed model.

The purposes of this study:

- To develop a hybrid FNN model integrating physics-based chemical corrosion model with inspection data for corrosion rate prediction.
- Implement Monte Carlo dropout to estimate uncertainty in the prediction of corrosion rates.
- To validate the model based on thickness time series and estimation of vessel RUL for different sections.

METHODOLOGY

Data sources

The dataset contains wall thickness measurements taken at 24 ultrasonic measurement points across different pressure vessel sections from 2002 to 2008 [12]. For each measurement, in addition to the historical record data, physics-based environmental data were generated to represent potential operating conditions. The simulated variables are as follows:

- Temperature (T)
- pH
- Concentration of Chloride ion (Cl⁻)
- Oxygen content (O₂)
- SO₄²⁻ concentration
- Fluid velocity (v)
- Ea: Activation of energy.
- Pre-exponential constants (K)
- Microbial Induced Corrosion (MIC)

These parameters are then the inputs of a physics-based corrosion model in which the corrosion rate (CR) is estimated. The model can be expressed as follows:

$$CR = K \cdot e^{\left(\frac{-E_a}{RT}\right)} \cdot f(pH) \cdot f(ion\ concentration) \cdot f(pressure) \cdot f(flow) \cdot f(MIC) \quad (1)$$

where R is the universal gas constant, T is the temperature in Kelvin, and f_pH, f_ion, f_pressure, f_flow, and f_MIC are correction factors representing the effects of pH, ionic species, pressure, fluid flow, and microbial activity, respectively [12].

This combined dataset (experimental thickness measurements and physics-based environmental data) was used to train and validate the machine learning model for corrosion rate prediction and remaining life estimation.

Neural Network Architecture

Using environmental and inspection data, a Feedforward Neural Network (FNN) model was established to predict the corrosion rates in pressure vessels. The FNN model has 11 input variables: temperature (T), pH, chloride ion concentration (Cl⁻), oxygen concentration (O₂), sulfate ion concentration (SO₄²⁻), fluid velocity (v), pressure (P), activation energy (E_a), pre-exponential rate constant (K), microbial-induced corrosion (MIC) and historical wall thickness (t_{past}). The FNN utilizes these explanatory variables in a three-hidden layer neural network architecture with 16, 8, and 4 neurons, followed by a single neuron output layer predicting corrosion rate (CR) in mm/year.

To further improve the generalization and produce estimates of uncertainty, dropout layers were placed following each of the hidden layers during the training and prediction. This provides the capability of Monte Carlo (MC) dropout to estimate the uncertainty in predictions from repeatable stochastic forward passes. The FNN model is illustrated in Fig. 1.

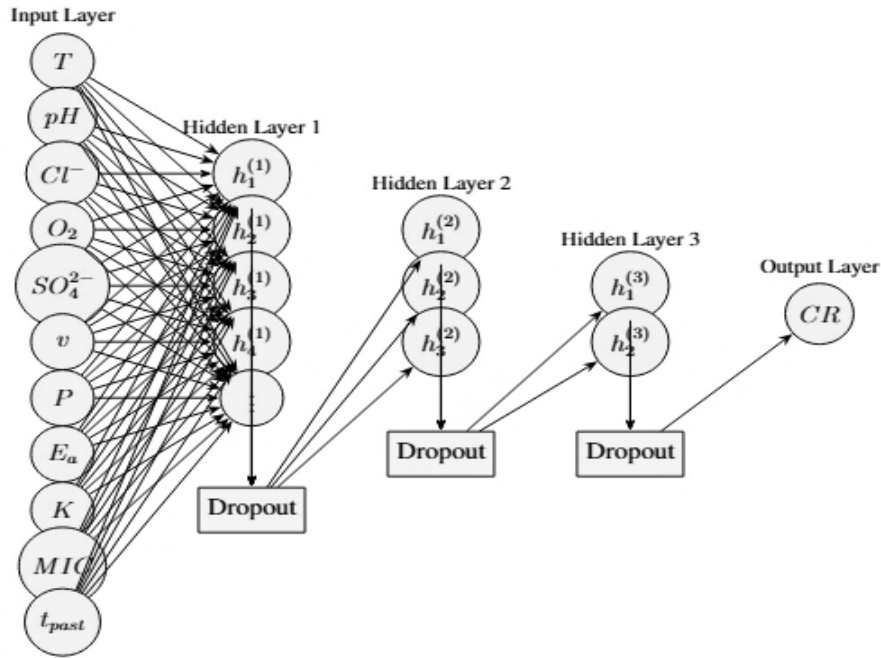


Figure 1: The hybrid feedforward neural network with MC Dropout for corrosion rate prediction.

Forward propagation equations

The equations below prescribe the forward propagation through the network:

- Hidden Layer Activations:

$$b^{(l)} = \sigma(w^{(l)} b^{(l-1)} + b^{(l)}) \quad (2)$$

where $h^{(l)}$ the activation of the l -th hidden layer (a vector of neuron outputs), σ is the ReLU activation function, defined as $\sigma(z) = \max(0, z)$, $w^{(l)}$ the weight matrix for the l -th layer (connects $h^{(l-1)}$ to $h^{(l)}$), $h^{(l-1)}$ the activation of the previous layer (or input variables for $l = 1$), and $b^{(l)}$ the bias vector for the l -th layer [13].

- ReLU Activation Function:

$$\sigma(z) = \max(0, z) \quad (3)$$

where z is the Input to the ReLU function (typically $w^{(l)} h^{(l-1)} + b^{(l)}$), $\sigma(z)$ is the output of the ReLU function, and all negative inputs are set to zero.

- Output Corrosion Rate:

$$CR = W^{(4)} b^{(3)} + b^{(4)} \quad (4)$$



where CR is the output corrosion rate (mm/year, scalar output), $W^{(4)}$ is the weight matrix for the output layer, $h^{(3)}$ is the activation of the third hidden layer, and $b^{(4)}$ is the bias vector for the output layer.

Exponential (Exp) Model Equation

The equation for the exponential model used to predict thickness degradation is presented [14] :

$$T(t) = T_0 \cdot \exp(-k \cdot t) \quad (5)$$

where $T(t)$ is the thickness at time t , T_0 is the initial thickness at the reference time (e.g., 2002), k is the decay rate constant fitted using curve fitting, and t is the time elapsed from the reference year (e.g., $t = \text{year} - 2002$)

Linear Model Equation

The linear model for thickness degradation is expressed as:

$$T(t) = T_0 - CR \cdot t \quad (6)$$

where $T(t)$ is the thickness at time t , T_0 is the initial thickness at the reference time (e.g., 2002), CR is the constant corrosion rate (mm/year) predicted by the FNN model, and t is the time elapsed from the reference year (e.g., $t = \text{year} - 2002$).

Mean squared error loss

The mean squared error (MSE) loss function used to train the FNN model is defined as:

$$L = \frac{1}{N} \sum (CR_i - \hat{CR}_i)^2, i = 1 \text{ to } N \quad (7)$$

where L is the loss value, N is the number of samples in the dataset, CR_i is the true corrosion rate for the i -th sample (mm/year), and \hat{CR}_i is the predicted corrosion rate for the i -th sample (mm/year)

Physics-based data generation

To enable robust model training across realistic operating variations, augmented environmental data were generated using a probabilistic sampling approach to augment the available inspection data. The inspection dataset consisted of wall thickness measurements from 24 measurement points across different vessel sections collected between 2002 and 2008, along with single-point measurements of operating conditions (temperature, pressure, pH, etc.). However, since only single-point measurements were available and the spatial and temporal variations in operating conditions within the vessel were not available, environmental parameters were sampled from distributions centered around the measured values and spanning typical industrial ranges reported in the corrosion kinetics literature [16] [17]. A total of 2000 scenarios were created to capture realistic operational variability, with each environmental variable sampled independently from either a normal or uniform distribution.

The sampling distributions were defined as follows: temperature (T) was sampled from a normal distribution with mean around 70°C and standard deviation up to 30°C; pH was uniformly sampled between 4 and 7; chloride ion concentration (Cl⁻) was sampled from a normal distribution with mean around 200 ppm and standard deviation up to 50 ppm; oxygen content (O₂) was uniformly sampled between 5 and 12 ppm; sulfate ion concentration (SO₄²⁻) was sampled from a normal distribution with mean around 50 ppm and standard deviation up to 15 ppm; fluid velocity (v) was uniformly distributed between 2 and 4 m/s; pressure (P) was sampled from a normal distribution with mean around 15 bar and standard deviation up to 5 bar; activation energy (E_a) was sampled from a normal distribution with mean around 75 kJ/mol and standard deviation up to 15 kJ/mol; and the pre-exponential rate constant (K) was sampled from a log-normal distribution with parameters about $\ln(10^6)$ and standard deviation around 0.5 to reflect the exponential sensitivity of corrosion kinetics. The historical wall thickness (t_{past}) from the 2002 inspection was included as an additional input feature for each vessel section. This physics-based dataset provides a diverse and statistically representative input space to train the corrosion prediction model under realistic environmental and operating conditions.

Neural network corrosion modelling using Dropout and Monte Carlo Dropout

Dropout is an important regularization approach for improving the generalization of a Feedforward Neural Network (FNN) that is used in the development of neural network models to predict corrosion rates in industrial components. In each



training iteration, dropout reduces the chance of overfitting the training dataset [16], which contains section-specific environmental parameter values such as temperature, chloride concentration, and historical thickness measurements, by randomly inactivating a fraction of neurons in the model. The underlying stochasticity encourages the model to learn more distributed and fewer neuron-specific features, leading to better generalization performance under new conditions. Dropout was applied in the model architecture immediately after each hidden layer (16, 8, and 4 neurons). This configuration balances the noise and variability in the inspection data and produces a stable corrosion rate prediction.

Moreover, MC Dropout is a Dropout enhancement during inference to quantify uncertainty, and it is an important feature desired for applications [17] requiring reliable corrosion rate estimates. By maintaining Dropout during prediction, the model returns multiple outputs for each input, with each prediction generated from a different subset of activated neurons [18]. These predictions yield the expected corrosion rate (mean), and the standard deviation provides the uncertainty in the predictions. By implementing the MC dropout prediction function, this method allows for section-level corrosion rate estimates, with confidence intervals displayed in the validation scatter plots and thickness prediction uncertainty bands. MC Dropout provides conservative estimates of the corrosion rates, helps interpret prediction uncertainty, and enhances the reliability of the vessel structural integrity assessment to support more informed decisions for corrosion mitigation.

DROPOUT EQUATION

The dropout operation randomly deactivates neurons during training by applying a Bernoulli mask to the activations [19] as follows:

$$r_j^{(l)} \sim \text{Bernoulli}(p) \tag{8}$$

$$\hat{a} = a \cdot r \tag{9}$$

where p is the probability of retaining a neuron, a is the activation vector, r is the Bernoulli mask (binary values), and \hat{a} is the masked activation.

Monte Carlo (MC) equation

MC Dropout prediction is implemented in the prediction function, which performs multiple stochastic forward passes to estimate the predictive mean and standard deviation [19]. The equations used are:

$$E(y|x) \approx \frac{1}{T} \sum_{t=1}^T f(x, \omega_t) \tag{10}$$

$$\text{std}(y|x) \approx \sqrt{\frac{1}{T} \sum_{t=1}^T f(x, \omega_t)^2 - \left(\frac{1}{T} \sum_{t=1}^T f(x, \omega_t)\right)^2} \tag{11}$$

where $f(x, \omega_t)$ is the output of the neural network at test time with dropout mask ω_t , and T is the number of stochastic forward passes.

To facilitate uncertainty quantification, the model integrates Dropout and Monte Carlo (MC) techniques. Dropout layers are applied after each hidden layer (16, 8, and 4 neurons), providing regularization during training and enabling Monte Carlo Dropout during inference. The uncertainty is estimated using the MC dropout prediction function, which performs multiple stochastic forward passes of the trained FNN model with dropout enabled. This technique quantifies epistemic uncertainty associated with model parameters. For the exponential thickness model, uncertainty in the fitted parameters (t_0 and k) is propagated to generate uncertainty bands in future thickness predictions. The predictive mean and standard deviation are calculated using Eqns. (10) and (11), producing uncertainty bands in the predicted thickness plots.

Environmental impact on corrosion

The effect of environmental conditions on corrosion plays a significant role in industrial component deterioration because it directs the amount and rate of deterioration of materials over time [20]. Corrosion is highly contingent upon the chemical and physical environments of the substrate, where the temperature, humidity, pH, chloride content, availability of oxygen, and fluid velocity all affect the rates of many processes. For example, the Arrhenius equation demonstrates the dependence of reaction rates on temperature [21], allowing the temperature effects to be captured in the chemical corrosion rate with simulated data [22]. In the model, high chloride levels favor ionic corrosion, especially in aqueous environments, whereas

high oxygen content or sulfide concentrations promote oxidation or sulfide corrosion mechanisms. Moreover, pressure, velocity, and pH also affect physical and chemical interactions at the material surface, potentially amplifying erosion-corrosion (E-C) effects [23]. Fig. 2 illustrates the effects of pH and temperature on corrosion rate, showing higher corrosion rates at lower pH values and elevated temperatures from the model.

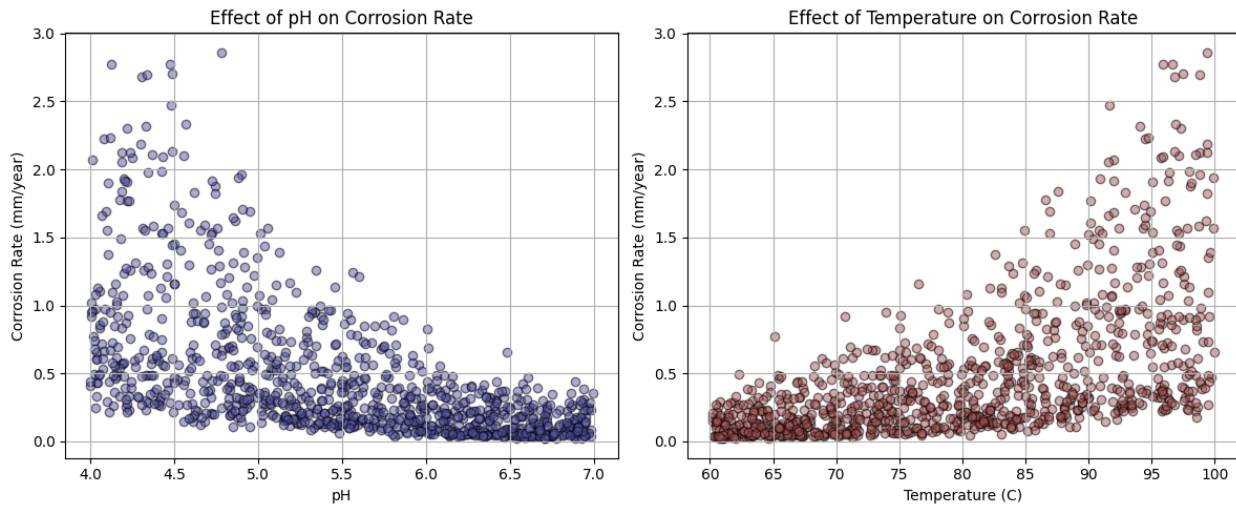


Figure 2: Environmental influence on corrosion rates from the physics-based model (a) Corrosion rate versus pH. (b) Corrosion rate versus temperature.

TRAINING

Dataset

This case study examines a corroded horizontal pressure vessel made of low-alloy steel (09G2s) operating in an industrial water environment. Wall thickness measurements were collected at 24 inspection points using ultrasonic testing (UT) from 2002 to 2008. The UT method provided reliable thickness data at designated grid points, as illustrated in Fig. 3.

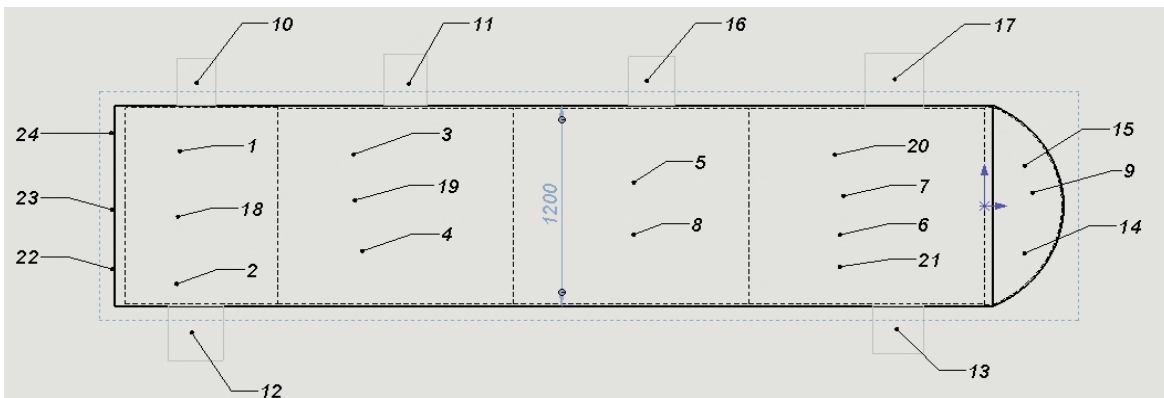


Figure 3: Vessel inspection points.

Section	Inspection Points	Section	Inspection Points
Shell 1	1, 2, 18	Nozzle A1	12
Shell 2	3, 4, 5, 6, 7, 8, 19, 20, 21	Nozzle N1	11
E Head 1	9, 14, 15	Nozzle N2	13
F Head 2	22, 23, 24	Nozzle N3	16
Nozzle A2	10	Nozzle N4	17

Table 1: Inspection points clusters.



Model training and prediction framework

The corrosion prediction model was developed through a four-stage approach combining chemical fundamentals, machine learning, and inspection data to estimate corrosion rates and remaining useful life (RUL).

Stage 1 - Simulated Data Generation: Environmental parameters (temperature, pH, chloride, oxygen, MIC, pressure, and flow velocity) were input into a modified Arrhenius-based chemical corrosion model (Eqn. 1) to generate training data representing realistic corrosion behavior under various operating conditions.

Stage 2 - FNN Training with MC Dropout: A feedforward neural network with three hidden layers was trained to predict corrosion rates using the 11 input features described earlier. Dropout layers were applied after each hidden layer to provide regularization during training and prevent overfitting. During inference, Monte Carlo dropout was implemented by keeping dropout active and performing multiple stochastic forward passes, generating both mean corrosion rate predictions and uncertainty estimates.

Stage 3 - Calibration with Inspection Data: The FNN predictions were calibrated using historical wall thickness measurements from 2002 to 2008. Exponential and linear degradation curves were fitted to the measured thickness data for each vessel section. The FNN predictions were adjusted using scaling factors derived from the observed thickness changes to ensure accurate section-specific predictions.

Stage 4 - RUL Estimation: The calibrated corrosion rates were used to project future wall thickness from 2008 to 2040. RUL for each vessel section was calculated as the time until predicted thickness reaches the minimum allowable threshold defined by design standards. Uncertainty bands were generated by propagating MC dropout uncertainties through the exponential thickness model parameters. Fig. 4 illustrates the complete workflow.

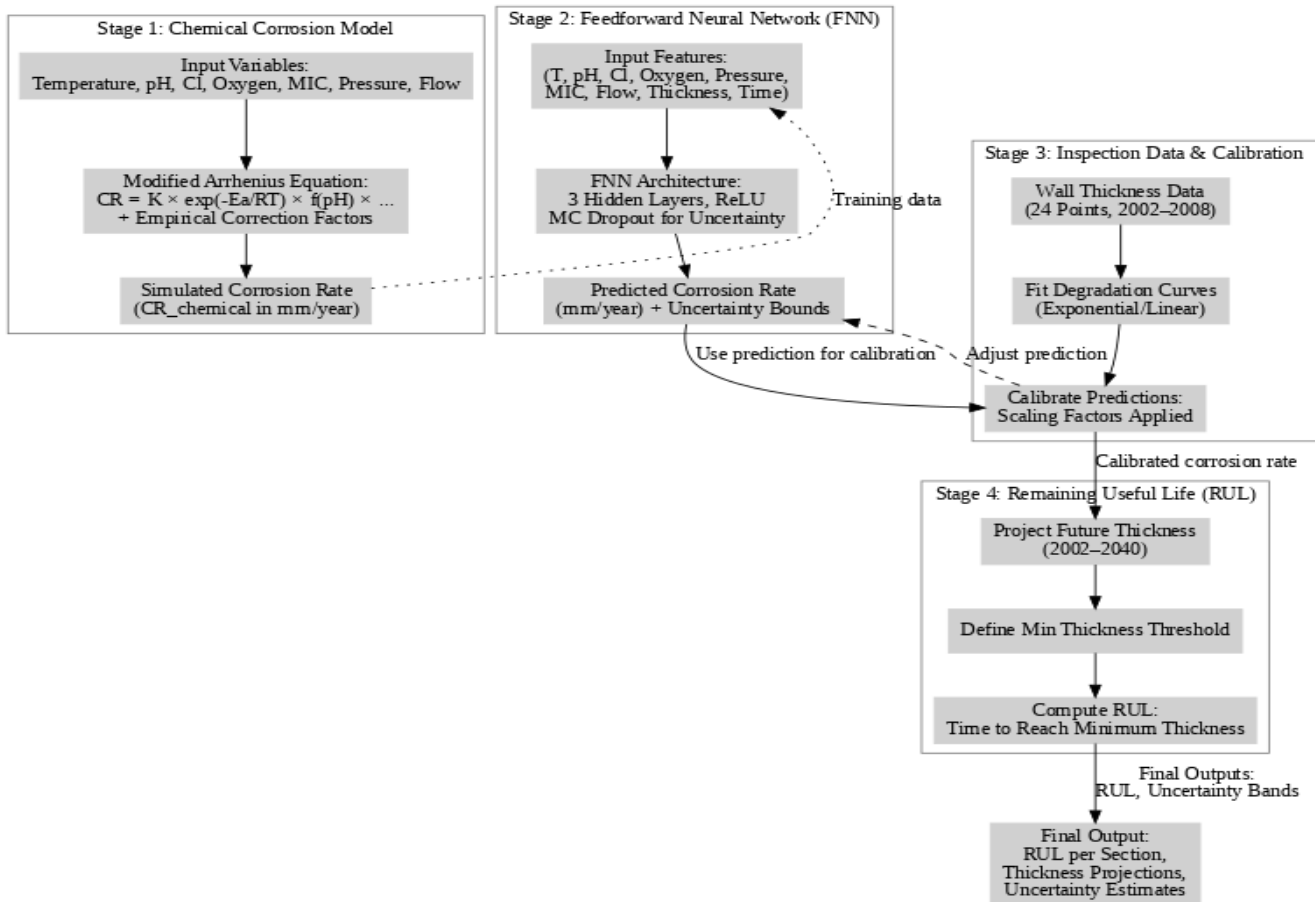


Figure 4: Feedforward Neural Network Model flowchart.

Evaluation metrics

Model performance was evaluated using standard error-based metrics for corrosion rate prediction with the FNN model and for thickness prediction using exponential and linear degradation models.



The Mean Squared Error (MSE)

$$MSE = \frac{1}{N} \sum (y_i - \hat{y}_i)^2 \quad (12)$$

The Mean Squared Error (MSE) is the loss function used to train models using the FNN architecture; it is the average squared difference between the actual values (y_i) and predicted values (\hat{y}_i), and N is the number of samples [24]. MSE is the loss function used to train the FNN, calculated as the average squared difference between actual and predicted corrosion rates over N samples. During training, MSE was minimized using the Adam optimizer. As a performance metric, MSE penalizes larger errors more heavily than smaller ones, which improves predictive accuracy for degradation trends. For corrosion rate predictions, the FNN achieved a test MSE of $0.02685 \text{ (mm/year)}^2$, demonstrating good convergence with inspection data. By minimizing MSE during optimization, the network learns to predict degradation curves more accurately, enabling improved remaining useful life estimation for each pressure vessel section.

Mean Absolute Error (MAE)

$$MAE = \frac{1}{N} \sum_{i=1}^N |y_i - \hat{y}_i| \quad (13)$$

MAE is the mean absolute error between predicted and actual values, providing an interpretable performance measure as it retains the units of the target variable (mm/year for corrosion rates). For corrosion rate predictions, the FNN achieved a test MAE of 0.12039 mm/year . This performance measure is suitable for real-world applications when determining the accuracy of predictions. MAE is important when evaluating whether and when maintenance thresholds are crossed, what sections are at risk, and their associated structural integrity in corrosive environments.

Root Mean Squared Error (RMSE)

$$RMSE = \sqrt{\frac{1}{N} \sum_{i=1}^N (y_i - \hat{y}_i)^2} \quad (14)$$

RMSE is the square root of MSE, providing an error measure in the original units while emphasizing larger errors. For corrosion rate predictions, the FNN achieved an RMSE of 0.1639 mm/year . RMSE was also used to compare the exponential and linear thickness degradation models, confirming that the exponential model provided more accurate thickness predictions.

Coefficient of Determination (R^2)

$$R^2 = 1 - \frac{\sum_{i=1}^N (y_i - \hat{y}_i)^2}{\sum_{i=1}^N (y_i - \bar{y})^2} \quad (15)$$

The Coefficient of Determination (R^2) is a measure of how well the model accounts for the variance in the data, as an R^2 value closer to 1 indicates a better fit for the model and explains the variance in the response variable [25]. For corrosion rates, the FNN had a test R^2 of 0.975 , confirming that the proposed model performed well in representing the degradation trends. For thickness predictions, the exponential degradation model achieved an overall R^2 of 0.99 , indicating excellent agreement with the measured wall thickness data across all vessel sections.

RESULTS AND DISCUSSION

Corrosion rate prediction

Prediction of the corrosion rate is one of the most important aspects when discussing the lifetime and performance of industrial components, while Fig. 6 presents an important comparison between the corrosion rates predicted by the Feedforward Neural Network (FNN) and the corrosion rates based on the inspection data. The FNN also shows a very competitive accuracy, with a Mean Absolute Error (MAE) of 0.12039 mm/year , which confirms its effectiveness for modelling corrosion dynamics. The application of Monte Carlo (MC) dropout even improves the robustness of the model, and bounds for uncertainties are on average one standard deviation from the mean prediction about 0.2 mm/year , indicating



a high confidence in the predictions. The solid tolerance banding of the data points shown in the figure confirms the robust validity of the model in terms of precision; hence, it is sufficiently sensitive enough in order to adequately mimic the degradation patterns of the sections.

Fig. 5 shows the FNN training history showing the convergence of training loss and validation loss over 500 epochs. Both losses decrease and stabilize, indicating effective model learning and good generalization to unseen data without overfitting. The graph shown is directly from a neural network model trained to predict corrosion rates on equipment used in industry based on past inspection data.

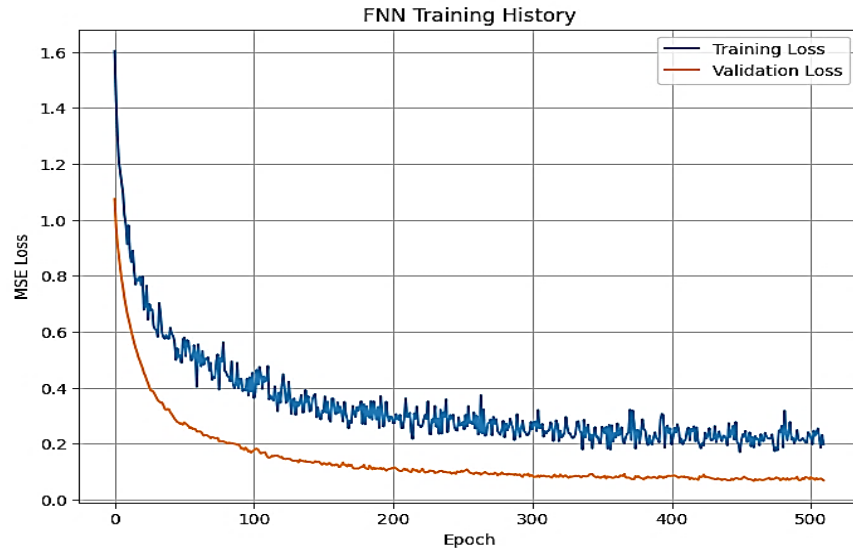


Figure 5: The loss of different models various with iterations.

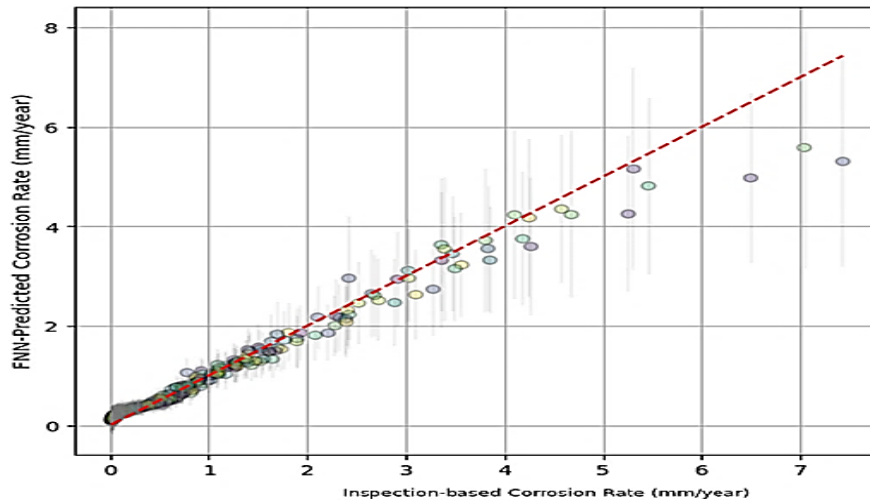


Figure 6: FNN-predicted versus inspection-based corrosion rate.

Thickness predictions

Thickness predictions are crucial for assessing the long-term performance of pressure vessel parts. The thickness predictions are shown in Fig. 7. It shows the predicted minimum wall thicknesses for all sections, historical wall thickness measurements from 2002 to 2008, and predictions to 2040 using both exponential and linear degradation models from the feedforward neural network (FNN). The exponential predicted model uses historical thickness measurements and Monte Carlo (MC) Dropout uncertainty to account for a conservative estimate of maximum loss in thickness (0.08 mm/year on average). The linear prediction model assumes a constant or average corrosion rate (0.10 mm/year) for all uniform reductions. Uncertainty bands and minimum allowable thickness lines were provided for sections E Head 1 and Nozzle N1, allowing engineers to effectively determine where critical sections can potentially monitor, repair, or replace to maintain structural integrity.

The figure shows time-series predictions for critical vessel sections (e.g., head, nozzle, and shell portions) and includes black dots with measured values from the years 2002–2008, red solid lines for the exponential predictions, blue dashed lines for the linear trends, red shaded areas for uncertainty bands (95% confidence), and green dashed lines for minimum thresholds.



The FNN-based exponential model predicted accurately with high fidelity to non-linear degradation or empirical corrosion-based observations, providing a more realistic risk-informed approach to predicting structural longevity than purely linear extrapolations that do not take into account the varying corrosion rates across components.

The model accuracy is evident based on the very small absolute error (typically <math><0.1\text{ mm}</math>) and relative errors (<math><1\%</math>), even with the highest relative error for Nozzle A1 of 1.25%, and all the errors for F Head 2 were very low, below 0.12%. These differences indicate that the models performed consistently regardless of section size and thickness, making it reasonable to have confidence in the predictive value of the exponential FNN representation for reliably predicting the long-term performance.

The linear model, although very simple, has the advantage of low complexity and presents an assumption of constant degradation over time, typically underpredicting or showing losses in future thicknesses (i.e., Nozzle N1, Shell 2), thus bringing into question the risks surrounding reliability-centered maintenance, especially at the minimum thresholds, as it did not include the uncertainty of those predictions. Finally, the exponential FNN showed a statistically significant improvement over the linear baseline, conforming more closely to realistic corrosion degradation patterns.

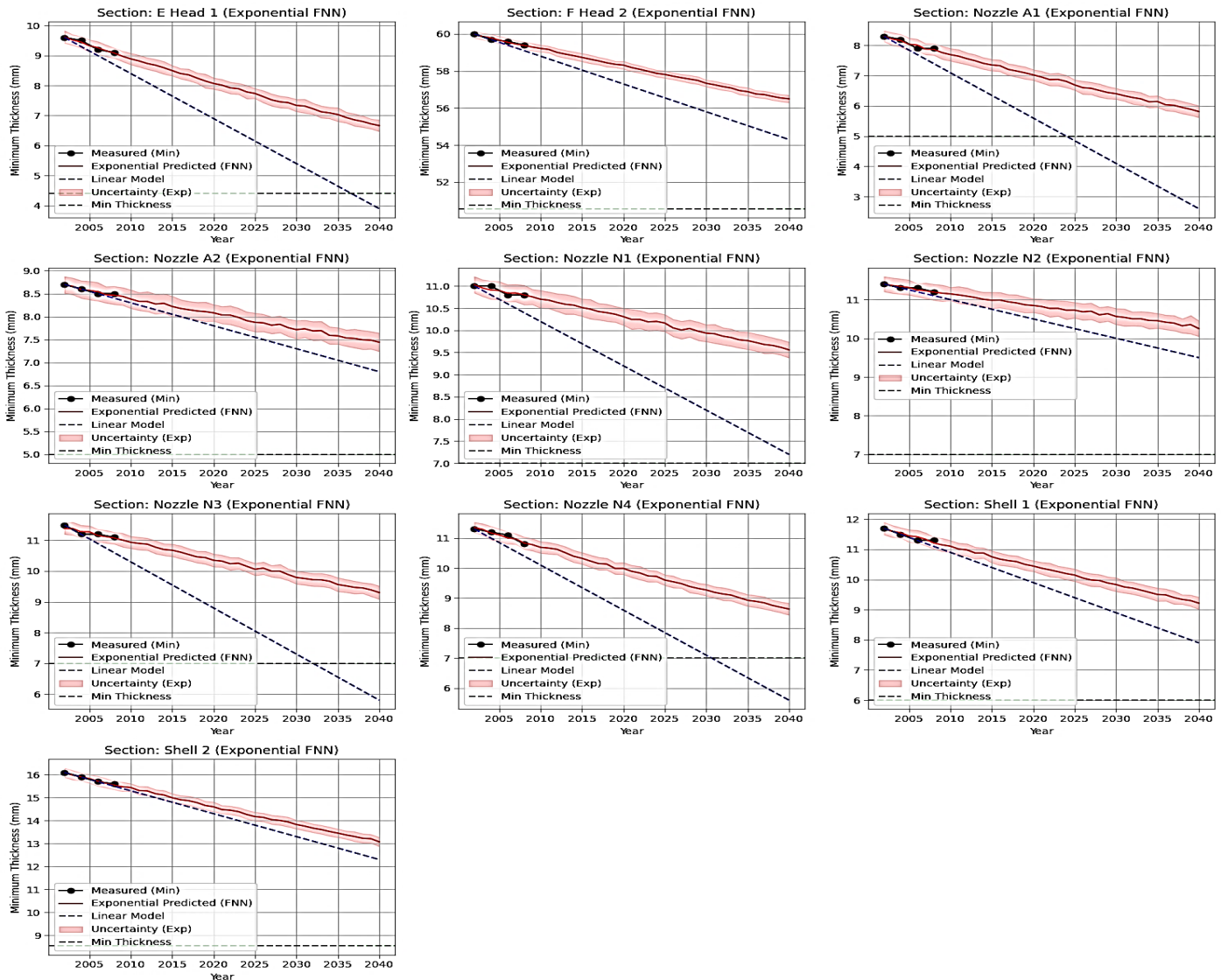


Figure 7: Thickness predictions for pressure vessel sections.

The anticipated minimum wall thickness trends across various sections of the pressure vessel, as shown in Fig. 7, show the historical data from 2002 to 2008 and the projected data to 2040. The exponential feedforward neural network (FNN) model provides a good fit to the measured data in a non-linear decaying pattern, which is consistent with the measured data and reflects the moderated corrosion rate with the later data range. The linear model implies a linear degradation rate and



produces a higher decline than the exponential model, particularly in the Nozzle A1 and E Head 1 sections, where the predicted thickness from the linear model falls below the minimum allowable thickness. The uncertainty bands around the exponential predictions based on a Monte Carlo dropout Monte Carlo uncertainty approach show relatively small uncertainty bands, demonstrating a high degree of confidence in the predictions and robustness of the model. Overall, this analysis is valuable for illustrating the linear versus exponential FNN modelling capabilities with respect to realistic and actual corrosion behaviors.

Model comparison statistics

Tab. 2 provides a structured comparison of the neural network exponential predictive model and the linear model using the summary statistics reported for the minimum thickness predictions over the ten structural sections. The statistics presented include the Mean Absolute Error (MAE), median absolute error, maximum absolute error, mean relative error, median relative error, and maximum relative error, and offer a quantitative measure of model performance at the section level.

Metric	Exponential FNN Model	Linear Model
Mean Absolute Error (mm)	0.0389	0.1350
Median Absolute Error (mm)	0.0301	0.1000
Max Absolute Error (mm)	0.1096	0.5000
Mean Relative Error (%)	0.3480	1.2458
Median Relative Error (%)	0.2562	0.4203
Max Relative Error (%)	1.2460	6.3291

Table 2: Exponential FNN vs. Linear Model Summary Statistics.

Estimation of the performance of the Exponential FNN model

Its corresponding section-level predictive performance as a function of time represents the absolute and relative errors separately and proves that the Exponential Feedforward Neural Network (FNN) model performs better in terms of both absolute and relative errors in modeling section-level structural degradation as per Fig. 8. The mean absolute error (MAE) is equal to 0.0389 mm, and the median absolute error is equal to 0.0301 mm, which shows that most of the predicted values differ from the measured values with a gap smaller than 0.04 mm. In most structural monitoring scenarios, such accuracy is important because even a slight underestimation or overestimation can impact maintenance decisions and risk assessment. In addition, the maximum absolute error is bounded by 0.1096 mm, so that all predicted values have the worst deviation within a narrow bound.

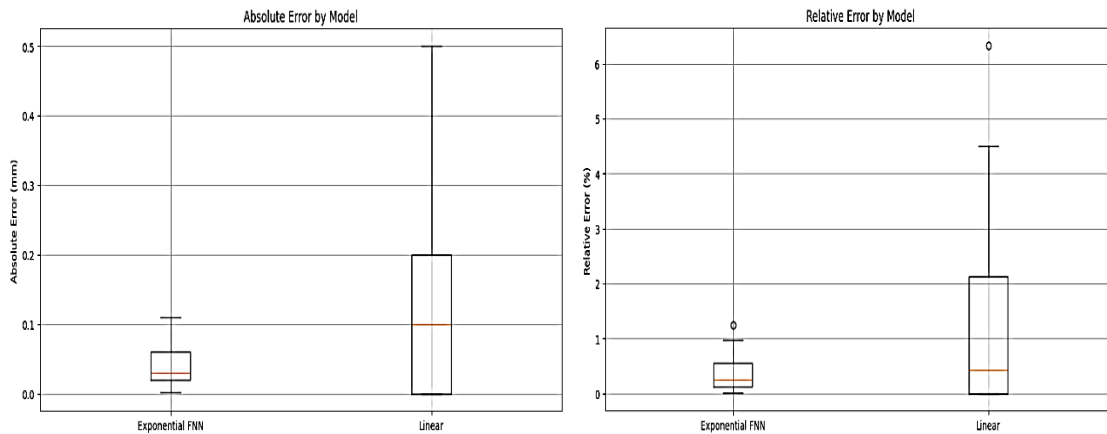


Figure 8: Statistical results of predictions by different models on the validation set. (a) shows the absolute error of different models, (b) shows the Relative error of different models.

The accuracy of the model was even clearer in the relative error metrics, observed a mean relative error of only 0.3480% and a median relative error of 0.2562%, indicating that the predictions were consistently proportional to the actual thickness measurements. The maximum relative error of 1.2460% is also low, and the R² value is 0.99, indicating a high degree of explained variance, confirming the model's accuracy.



In comparison with the linear Model, it shows significantly higher errors with a mean absolute error of 0.1350 mm (3.5 times higher) and a mean relative error of 1.2458% (3.6 times higher), thus the Exponential FNN model demonstrates better performance with lower error rates across all metrics.

This result demonstrates that the exponential FNN model accurately tracks the actual degradation path of structural elements. The exponential decay formulation is particularly appropriate for structures undergoing erosion or corrosion processes, where degradation rates typically decrease over time as protective oxide layers form or reactive species are depleted. By aligning with observed degradation trends, this approach provides confidence in the model for long-term prediction, remaining useful life estimation, and determining optimal inspection intervals.

FITNESS-FOR-SERVICE (FFS) AND STRUCTURAL INTEGRITY ASSESSMENT

To evaluate remaining useful life (RUL) across different vessel sections, both linear and exponential degradation models were applied. The linear model assumes constant corrosion rates over time, representing conservative worst-case scenarios. The exponential model captures nonlinear degradation behavior influenced by environmental factors and protective mechanisms. Both models were used to predict future thickness and assess structural integrity according to ASME Section VIII and API 579-1 standards [26].

Determine minimum required wall thickness

The minimum allowable wall thickness (t_{min}) for each vessel section was calculated according to ASME Section VIII and API 579-1/ASME FFS-1 [27], accounting for design pressure, material properties, and safety factors.

Level 1 acceptance criteria for minimum measured thickness

$$t_{mm} - FCA \geq \max (0.5t_{min} , t_{lim}) \tag{16}$$

$$t_{lim} = \max (0.2t_{nom} , 2.5) \tag{17}$$

where t_{mm} is the minimum measured thickness, FCA is the future corrosion allowance (corrosion rate \times future service period), t_{min} is the minimum required thickness, and t_{nom} is the nominal thickness [27].

Calculating remaining life

$$Remaining\ life = \frac{t_{initial} - t_{min}}{CR} \tag{18}$$

where $t_{initial}$ is the initial thickness of the material (mm), t_{min} minimum allowable thickness (mm) determined by fitness-for-service criteria, and CR is the corrosion rate (mm/year) [28].

Section	t_{mm}	t_{min}	Min Predicted Thickness (2040)	Status
E Head 1	9.1	4.5	6.7	SAFE
F Head 2	59.4	50.6	56.4	SAFE
Nozzle A1	7.9	5.0	5.8	SAFE
Nozzle A2	8.5	5.0	7.4	SAFE
Nozzle N1	10.8	7.0	9.6	SAFE
Nozzle N2	11.2	7.0	10.3	SAFE
Nozzle N3	11.1	7.0	9.3	SAFE
Nozzle N4	10.8	7.0	8.6	SAFE
Shell 1	11.3	6.0	9.2	SAFE
Shell 2	15.6	8.5	13.1	SAFE

Table 4: Exponential model predicted thickness.



Section	t_{mm}	t_{min}	Min Predicted Thickness (2040)	Status
E Head 1	9.10	4.5	3.90	UNSAFE
F Head 2	59.40	50.6	54.30	SAFE
Nozzle A1	7.90	5.0	2.60	UNSAFE
Nozzle A2	8.50	5.0	6.80	SAFE
Nozzle N1	10.80	7.0	7.20	SAFE
Nozzle N2	11.20	7.0	9.50	SAFE
Nozzle N3	11.10	7.0	5.80	UNSAFE
Nozzle N4	10.80	7.0	5.60	UNSAFE
Shell 1	11.30	6.0	7.90	SAFE
Shell 2	15.60	8.5	12.30	SAFE

Table 5: Linear model predicted thickness.

The exponential model as per Tab. 4 predicts that all vessel sections will remain above the minimum allowable thickness (t_{min}) through 2040, indicating SAFE status for all components. This model accounts for decreasing corrosion rates over time due to protective film formation and environmental stabilization. For example, E Head 1 shows a predicted thickness of 6.7 mm compared to t_{min} of 4.5 mm, providing adequate safety margin. Thicker sections such as F Head 2 demonstrate minimal relative thickness loss, supporting the validity of the exponential model for long-term predictions.

The linear model as per Tab. 5 applies constant corrosion rates and predicts UNSAFE conditions for four sections: E Head 1 (3.9 mm < 4.5 mm), Nozzle A1 (2.6 mm < 5.0 mm), Nozzle N3 (5.8 mm < 7.0 mm), and Nozzle N4 (5.6 mm < 7.0 mm). This conservative approach is appropriate for worst-case scenario planning and identifies sections requiring priority inspection and potential mitigation measures. Thicker sections such as F Head 2 remain SAFE under both models, confirming adequate structural integrity for these components.

SUMMARY OF PREDICTION MODELS

The following Tab. 6 summarizes the proposed and selected studies, highlighting their methodologies and performance metrics.

Study	Model Type	Data Used	Architecture/Method	Performance	Remarks
Proposed Study	Hybrid FNN + Physics-based Model	Environmental variables and NDE thickness measurements obtained (2002-2008, 24 inspection points)	3-layer FNN (16-8-4 neurons) with Monte Carlo Dropout and exponential degradation model	Corrosion Rate Prediction $R^2 = 0.975$ MSE = 0.02685 MAE = 0.12039 Thickness prediction $R^2 = 0.99$ MAE = 0.0389 mm, Max AE = 0.1096 mm, Relative Error = 0.3480%	High accuracy with uncertainty quantification; exponential model outperforms linear baseline for thickness prediction with lower MAE and relative error



Study	Model Type	Data Used	Architecture/Method	Performance	Remarks
Tiwari et al. (2025) [29]	Machine Learning (Linear Regression, Random Forest, Gradient Boosting)	Scientifically informed physics-based dataset based on ISO 9223 standards and peer-reviewed literature	Three regression models; Gradient Boosting with feature importance analysis (copper content 30%, exposure time 20%, chloride deposition 15%)	$R^2 = 0.835 \pm 0.024$ RMSE = 98.99 ± 16.62 $\mu\text{m}/\text{year}$	Superior performance by Gradient Boosting; significant for protective coating design and infrastructure risk assessment; requires experimental validation
Wang et al. (2022) [9]	Principal component analysis + Multi-Layer Perceptron Neural Network (PCA-MLPNN)	Corrosion data simulated by De Waard 95 model in OLGA for submarine multiphase flow pipelines	PCA for dimensionality reduction + MLPNN; compared with MLR, RBFNN, PCA-MLR, PCA-RBFNN	$R^2 = 0.8609$ RMSE = 0.0082 MAE = 0.0034 Average Relative Error = 3.318%	Higher prediction accuracy with PCA-MLPNN; reliable for CO2 corrosion prediction in submarine pipelines
Lu et al. (2023) [30]	Hybrid Physics with Machine Learning	CFD-based pipeline corrosion dataset for O ₂ and CO ₂	Hybrid model integrating CFD and LightGBM. Uses four variables (inlet velocity, pipe ID, bend angle, bend radius/pipe ID ratio)	$R^2 = 0.9816$, MSE = 2.4165 (test) $R^2 = 0.9958$, MSE = 0.3561 (validation) $R^2 = 0.9591$, MSE = 6.1717 (10-fold cross validation)	Faster than CFD high accuracy predictive corrosion of CO ₂ and O ₂ ; reduces variables required for modelling.
Obaseki & Elijah (2021) [31]	Artificial Neural Network (ANN)	Pipeline corrosion data influenced by pH, temperature, and other physical parameters	ANN model compared with De Waard model; validated for corrosion in acidic environments	$R^2 = 0.9521$, RMSE = 0.0130 MAE = 0.0079 Scattered Index = 0.1708, Relative Error = 0.013%–0.047%	High prediction accuracy (>95%); robust for acidic corrosion environments; consistent with experimental and De Waard model results
Zakikhani et al. (2020) [32]	Multiple regression analysis	Historical data of gas transmission pipelines in Great Plains and South East U.S. regions.	Multiple regression models developed examining external corrosion, scenario-based analysis with diagnostic procedures and residual analysis.	$R^2 = 0.93$ (Great Plains) RMSE = 0.04 (Great Plains) $R^2 = 0.75$ (South East) RMSE = 0.07 (South East)	Potential to be useful for planning maintenance, considers environmental and geographical variables, and estimates the predicted failure due to external corrosion.
Jiménez-Come et al. (2023)[33]	Artificial neural network (ANN)	Experimental data applying stainless steel in biogas environments (composition, temperature, surface finish, breakdown potential).	ANN with materials composition and breakdown potential predicting corrosion status with no need for microscopic analysis.	Accuracy = 0.966 Specificity = 0.969 Sensitivity = 0.971	Useful for predicting localized corrosion in the production of biogas; will be applicable to the design and maintenance of stainless steel structures.
Hu (2024) [34]	Ensemble Machine Learning	Corrosion data of oil and gas pipelines after feature	(ExtraTreeRegression) with SHAP for interpretability and	$R^2 = 0.93$	Internal corrosion rate prediction; identifies



Study	Model Type	Data Used	Architecture/Method	Performance	Remarks
	(ExtraTreeRegression)	engineering and preprocessing	ALE for feature effects. Compared to other models such as : RF, AdaBoost, GBRT, XGBoost, CatBoos		temperature, pressure, and CO ₂ partial pressure as key factors. Outperforms other models in accuracy.
Diao et al. (2021) [35]	Machine Learning (Random Forest)	Marine corrosion data of low-alloy steels (chemical composition and environmental factors)	Random Forest with feature reduction (GBDT, Kendall correlation, PCA) and feature creation (atomic and physical properties)	Method II: Training RMSE = 0.019 R ² = 0.91 Test RMSE = 0.022 R ² = 0.90	Improves generalization by converting chemical features to atomic/physical properties; R ² > 0.9. Applicable to seawater corrosion resistance evaluation
Liu & Meng (2025) [24]	ANN with empirical formula	Simulated burst tests taken from literature	4-layer ANN with an empirical formula (DNV RP-F101) restrained loss function	R ² = 0.9886 MAPE = 2.52%; RMSE = 0.39 MPa	Integrated empirical knowledge with the ANN loss function. Improved accuracy for prediction for failure pressure in corroded pipelines.

Table 6: Review of Data-Driven and Hybrid Models.

The comparison reveals that different models excel at specific prediction tasks. Liu and Meng (2025) developed a physics-informed neural network for predicting failure pressure of corroded pipelines, incorporating the DNV RP-F101 empirical formula into the loss function. Their model achieved strong accuracy with MAPE = 2.52% and R² = 0.9886 on 60 burst test samples, demonstrating the effectiveness of integrating empirical knowledge with neural networks for failure pressure prediction. The model proposed in this study provides a broader assessment framework by predicting corrosion rates (R² = 0.975), future thickness degradation (MAE = 0.0389 mm), and remaining useful life while quantifying uncertainty through Monte Carlo dropout.

The hybrid approach combines a physics-based exponential degradation model with a data-driven feedforward neural network, providing both point estimates and confidence intervals for maintenance planning. Compared to other corrosion rate prediction studies, such as Wang et al. (2022) with R² = 0.8609 and Obaseki & Elijah (2021) with R² = 0.9521, the proposed model demonstrates acceptable predictive performance. Additionally, the exponential thickness prediction model achieves low errors (MAE = 0.0389 mm, relative error = 0.348%), outperforming the linear baseline across all metrics. The integrated framework enables comprehensive vessel condition assessment, predicting both current and future degraded states with uncertainty quantification, which supports informed decision-making for maintenance planning and risk management.

CONCLUSION

This study demonstrates a hybrid feedforward neural network (FNN) model integrated with a physics-based corrosion model for predicting corrosion rates and estimating the remaining useful life (RUL) of pressure vessels. Using non-destructive evaluation (NDE) 24 thickness measurements from different sections (2002–2008) and physics-based training data, the three-layer FNN model with Monte Carlo dropout achieved R² = 0.975 for corrosion rate prediction. The model achieved MSE = 0.02685 (mm/year)² and MAE = 0.120 mm/year for corrosion rate predictions.

For thickness prediction, the exponential degradation model outperformed the linear baseline, achieving over all R² = 0.99 across all sections, MAE = 0.0389 mm, maximum absolute error = 0.1096 mm, and mean relative error = 0.3480%. The exponential model captures the nonlinear nature of corrosion degradation, providing more realistic thickness projections than traditional linear models that assume constant corrosion rates.

The model predictions were integrated into a Fitness-for-Service (FFS) assessment framework based on API 579-1/ASME FFS-1 standards. By comparing predicted future thickness against minimum allowable thickness (t_{min}), components were categorized as "SAFE" or "UNSAFE". The analysis showed that while the linear model flagged several components as potentially requiring mitigation due to its conservative constant-rate assumption, the exponential model provided a less conservative long-term assessment while maintaining structural integrity requirements. This approach translates predictive



analytics into standards-compliant integrity assessments, supporting practical engineering decision-making for condition-based maintenance planning.

SCOPE AND FUTURE WORK

This study demonstrates a hybrid neural network approach for corrosion prediction in pressure vessels using physics-based training data and historical inspection measurements. Several areas for future investigation are identified.

Data Expansion: The current model was validated using 24 thickness measurements from different sections over a six-year period (2002-2008) and physics-based environmental parameters. Future work should incorporate real-time environmental monitoring data and extend validation to longer inspection intervals. Expanding the dataset to include additional vessel geometries and operating conditions would further assess model generalizability.

Model Generalization: The current model is calibrated to a specific pressure vessel asset. Future research could adapt this framework to multiple assets with varying material properties, fluid compositions, and operating environments. This would require developing transfer learning approaches or ensemble methods to maintain accuracy across diverse corrosion scenarios.

Environmental Parameter Refinement: The physics-based corrosion model incorporates temperature, pH, chloride, oxygen, sulfate, MIC, pressure, and flow velocity. Future work could investigate additional parameters such as CO₂ partial pressure, H₂S concentration, and stress corrosion cracking factors to improve prediction accuracy in specific industrial applications.

Uncertainty Quantification: While Monte Carlo dropout provides prediction uncertainty estimates, future work could explore alternative Bayesian approaches or ensemble methods to better characterize epistemic and aleatoric uncertainty in corrosion predictions.

FUNDING INFORMATION

This research did not receive any specific grant from funding agencies in the public, commercial, or not-for-profit sectors.

DECLARATION OF CONFLICT

The author declare that they have no known competing financial interests or personal relationships that could have appeared to influence the work reported in this paper.

USE OF AI AND AI-ASSISTED TECHNOLOGIES

During the preparation of this manuscript, the author used Google Colab as the computational environment for implementing and training the feedforward neural network model, and Paperpal for language improvement. After using these tools, the author reviewed and edited the content as needed and take full responsibility for the content of the publication.

REFERENCES

- [1] Rajendran, M. and Subbian, D. (2025). Deep learning in corrosion assessment and control: a critical review of techniques and challenges, *Corrosion Reviews*. DOI: <https://doi.org/10.1515/corrrev-2024-0060>.
- [2] Wang, M.-O. and Dai, S.-H. (1989). A Study of Reliability Assessment in Pressure Vessel Applications, *Design & Analysis*, pp. 1493–1500. DOI: 10.1016/B978-1-4832-8430-9.50140-4.



- [3] Wang, Q., Song, Y., Zhang, X., Dong, L., Xi, Y., Zeng, D., Liu, Q., Zhang, H., Zhang, Z., Yan, R., Luo, H. (2023). Evolution of corrosion prediction models for oil and gas pipelines: From empirical-driven to data-driven, *Eng Fail Anal*, 146, p. 107097. DOI: <https://doi.org/10.1016/j.engfailanal.2023.107097>.
- [4] Yarveisy, R., Khan, F. and Abbassi, R. (2022). Data-driven predictive corrosion failure model for maintenance planning of process systems, *Comput Chem Eng*, 157, p. 107612. DOI: <https://doi.org/10.1016/j.compchemeng.2021.107612>.
- [5] Coelho, L.B., Zhang, D., Van Ingelgem, Y., Steckelmacher, D., Nowé, A. and Terry, H. (2022). Reviewing machine learning of corrosion prediction in a data-oriented perspective, *Npj Mater Degrad*, 6(1), p. 8. DOI: <https://doi.org/10.1038/s41529-022-00218-4>.
- [6] Zhang, Z. and Sun, C. (2021). Structural damage identification via physics-guided machine learning: a methodology integrating pattern recognition with finite element model updating, *Struct Health Monit*, 20(4), pp. 1675–1688. DOI: <https://doi.org/10.1177/1475921720927488>.
- [7] Silva, R.C.C., Guerreiro, J.N.C. and Loula, A.F.D. (2007). A study of pipe interacting corrosion defects using the FEM and neural networks, *Advances in Engineering Software*, 38(11–12), pp. 868–875. DOI: <https://doi.org/10.1016/j.advengsoft.2006.08.047>.
- [8] Mehri Sofiani, F., Tacq, J., Elahi, S.A., Chaudhuri, S. and De Waele, W. (2024). A hybrid probabilistic-deterministic framework for prediction of characteristic size of corrosion pits in low-carbon steel following long-term seawater exposure, *Corros Sci*, 232, p. 112039. DOI: <https://doi.org/10.1016/j.corsci.2024.112039>.
- [9] Wang, G., Wang, C. and Shi, L. (2022). CO₂ Corrosion Rate Prediction for Submarine Multiphase Flow Pipelines Based on Multi-Layer Perceptron, *Atmosphere (Basel)*, 13(11), p. 1833. DOI: <https://doi.org/10.3390/atmos13111833>.
- [10] Ma, Y., Zheng, J., Liang, Y., Klemeš, J. J., Du, J., Liao, Q., Lu, H., Wang, B. (2022). DeepPIPE: Theory-guided neural network method for predicting burst pressure of corroded pipelines, *Process Safety and Environmental Protection*, 162, pp. 595–609. DOI: <https://doi.org/10.1016/j.psep.2022.04.036>.
- [11] Shabani, M., Kadoch, M. and Mirjalili, S. (2025). A novel metaheuristic-based approach for prediction of corrosion characteristics in offshore pipelines, *Eng Fail Anal*, 170, p. 109231. DOI: <https://doi.org/10.1016/j.engfailanal.2024.109231>.
- [12] Pascal, M.A., Sultanmagomedov, T. and Magomedtagirovich, S. (2025). Prediction models for remaining life assessment of Pressure Vessels: A comparative analysis of inspection-based and chemical approaches, *Journal of Integrated Science and Technology*, 13(6), p. 1136. DOI: <https://doi.org/10.62110/sciencein.jist.2025.v13.1136>.
- [13] Heaton, J. (2018). Ian Goodfellow, Yoshua Bengio, and Aaron Courville: Deep learning, *Genet Program Evolvable Mach*, 19(1–2), pp. 305–307. DOI: <https://doi.org/10.1007/s10710-017-9314-z>.
- [14] Li, Z., Ma, W., Gan, Y. and Zhong, D. (2025). Deciphering chlorine decay influenced by corrosion scale and biofilm from pipe walls in water distribution system: A variable rate exponential model, *Journal of Water Process Engineering*, 75, p. 107910. DOI: <https://doi.org/10.1016/j.jwpe.2025.107910>.
- [15] Liu, J., Zhang, T., Zhang, W., Yang, Y.-G., Shao, Y.-W., Meng, G.-Z. and Wang, F.-H. (2015). Quantitative Modeling for Corrosion Behavior in Complex Coupled Environment by Response Surface Methodology, *Acta Metallurgica Sinica (English Letters)*, 28(8), pp. 994–1001. DOI: <https://doi.org/10.1007/s40195-015-0286-9>.
- [16] Srivastava, N., Hinton, G., Krizhevsky, A. and Salakhutdinov, R. (2014). Dropout: A Simple Way to Prevent Neural Networks from Overfitting, *Journal of Machine Learning Research*, 15, pp. 1929–1958.
- [17] Hernández, S., Vergara, D., Valdenegro-Toro, M. and Jorquera, F. (2020). Improving predictive uncertainty estimation using Dropout–Hamiltonian Monte Carlo, *Soft comput*, 24(6), pp. 4307–4322. DOI: <https://doi.org/10.1007/s00500-019-04195-w>.
- [18] Daday, M.J.A., Fajardo, A.C. and Medina, R.P. (2019). Enhancing Feed-Forward Neural Network in Image Classification. *Conference on Computing and Big Data*, New York, USA. DOI: <https://doi.org/10.1145/3366650.3366651>.
- [19] Gal, Y. and Ghahramani, Z. (2016). Dropout as a Bayesian Approximation: Representing Model Uncertainty in Deep Learning. *International Conference on Machine Learning*, New York, 20–22 June. Available at: <http://arxiv.org/abs/1506.02142>.
- [20] Klimesmith, D.E., McCuen, R.H. and Albrecht, P. (2007). Effect of Environmental Conditions on Corrosion Rates, *Journal of Materials in Civil Engineering*, 19(2), pp. 121–129. DOI: [https://doi.org/10.1061/\(ASCE\)0899-1561\(2007\)19:2\(121\)](https://doi.org/10.1061/(ASCE)0899-1561(2007)19:2(121)).
- [21] Kamrunnahar, M. and Urquidí-Macdonald, M. (2011). Prediction of corrosion behaviour of Alloy 22 using neural network as a data mining tool, *Corros Sci*, 53(3), pp. 961–967. DOI: <https://doi.org/10.1016/j.corsci.2010.11.028>.
- [22] Shukla, S.K. and Ebenso, E.E. (2011). Corrosion Inhibition, Adsorption Behavior and Thermodynamic Properties of Streptomycin on Mild Steel in Hydrochloric Acid Medium, *Int J Electrochem Sci*, 6(8), pp. 3277–3291.



- DOI: [https://doi.org/10.1016/S1452-3981\(23\)18251-4](https://doi.org/10.1016/S1452-3981(23)18251-4).
- [23] Tang, P., Yang, J., Zheng, J.Y., Lam, C.K., Wong, I. and He, S.Z. (2009). Predicting Erosion-Corrosion Induced by the Interactions Between Multiphase Flow and Structure in Piping System, *J Press Vessel Technol*, 131(6). DOI: <https://doi.org/10.1115/1.4000063>.
- [24] Liu, H. and Meng, X. (2025). Prediction of Corroded Pipeline Failure Pressure Based on Empirical Knowledge and Machine Learning, *Applied Sciences*, 15(10), p. 5787. DOI: <https://doi.org/10.3390/app15105787>.
- [25] Xu, L., Wen, S., Huang, H., Tang, Y., Wang, Y. and Pan, C. (2025). Corrosion failure prediction in natural gas pipelines using an interpretable XGBoost model: Insights and applications, *Energy*, 325, p. 136157. DOI: <https://doi.org/10.1016/j.energy.2025.136157>.
- [26] Zangeneh, Sh., Lashgari, H.R. and Sharifi, H.R. (2020). Fitness-for-service assessment and failure analysis of AISI 304 demineralized-water (DM) pipeline weld crack, *Eng Fail Anal*, 107, p. 104210. DOI: <https://doi.org/10.1016/j.engfailanal.2019.104210>.
- [27] Nakasone, Y. and Konosu, S. (2023). Key Considerations in Fitness-for-Service Assessment Procedures, *Journal of Failure Analysis and Prevention*, 23(6), pp. 2661–2672. DOI: <https://doi.org/10.1007/s11668-023-01805-6>.
- [28] Jayanto, S.T., Chendra, M. and Wijayanta, A.T. (2019). Estimating corrosion rate and remaining life of a pressure vessel of H2S absorber. *AIP Conference Proceedings*, 2097(1). DOI: <https://doi.org/10.1063/1.5098182>.
- [29] Tiwari, S., Dash, K., Park, N. and Reddy, N.G.S. (2025). Machine Learning-Based Prediction of Atmospheric Corrosion Rates Using Environmental and Material Parameters, *Coatings*, 15(8), p. 888. DOI: <https://doi.org/10.3390/coatings15080888>.
- [30] Yang, H., Lu, L., Tsai, K. and Sidahmed, M. (2023). A Hybrid Physics and Active Learning Model For CFD-Based Pipeline CO₂ and O₂ Corrosion Prediction. *International Petroleum Technology Conference, IPTC*, Bangkok, Thailand, March. DOI: <https://doi.org/10.2523/IPTC-23049-EA>.
- [31] Obaseki, M. and Elijah, P.T. (2021). Application of Artificial Neural Network Model to Predict Corrosion Rates on Pipeline, *Journal of Newviews in Engineering and Technology (JNET)*, 3(2). Available at: <http://www.rsujnet.org/index.php/publications/2021-edition>.
- [32] Zakikhani, K., Nasiri, F. and Zayed, T. (2021). A failure prediction model for corrosion in gas transmission pipelines, *Proc Inst Mech Eng O J Risk Reliab*, 235(3), pp. 374–390. DOI: <https://doi.org/10.1177/1748006X20976802>.
- [33] Jiménez-Come, M.J., González Gallero, F.J., Álvarez Gómez, P. and Mena Baladés, J.D. (2023). Corrosion Behaviour Modelling Using Artificial Neural Networks: A Case Study in Biogas Environment, *Metals (Basel)*, 13(11), p. 1811. DOI: <https://doi.org/10.3390/met13111811>.
- [34] Hu, J. (2024). Prediction of the internal corrosion rate for oil and gas pipelines and influence factor analysis with interpretable ensemble learning, *International Journal of Pressure Vessels and Piping*, 212, p. 105329. DOI: <https://doi.org/10.1016/j.ijpvp.2024.105329>.
- [35] Diao, Y., Yan, L. and Gao, K. (2021). Improvement of the machine learning-based corrosion rate prediction model through the optimization of input features, *Mater Des*, 198, p. 109326. DOI: <https://doi.org/10.1016/j.matdes.2020.109326>.